

H1 Diffractive Structure Function Measurements and QCD Fits

S. Schätzel^{a*} (for the H1 Collaboration)

^aPhysikalisches Institut, Philosophenweg 12, D-69120 Heidelberg, Germany

Measurements of diffractive structure functions in ep collisions and diffractive parton densities extracted from QCD fits are presented.

1. DIFFRACTION AT HERA

At the HERA ep collider the diffractive quark structure of the proton is probed with a point-like photon (Fig. 1). The virtuality of the photon

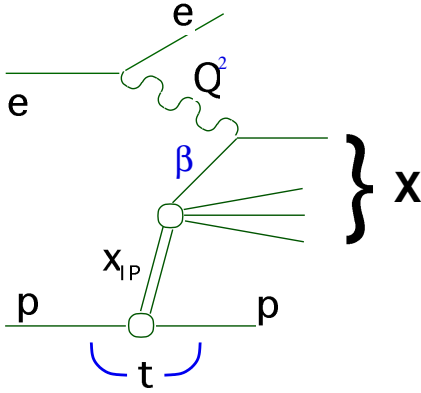


Figure 1. Diffractive ep scattering.

is denoted by Q^2 and sets the hard scale of the interaction. Diffraction is characterised by an elastically scattered proton which loses only a small fraction x_P of its initial beam momentum. These events are selected experimentally by detecting the proton at small scattering angles (roman pot detectors) or by requiring a large empty area in the detector between the outgoing proton and the hadronic system X produced in the interaction (rapidity gap). The squared 4-momentum t transferred at the proton vertex can be measured by tagging the proton. For the rapidity gap method, which accesses a much larger

event sample, the cross section has to be integrated over $|t| < 1 \text{ GeV}^2$ and in $\approx 10\%$ of the events the proton is excited into a hadronic system of small mass $< 1.6 \text{ GeV}$. The two methods give the same results when compared in the same kinematic range.

In a picture which depicts diffraction as a two step process, the proton exchanges a diffractive object (often called the pomeron) with momentum fraction x_P and the quark struck by the photon carries a fraction β of the momentum of the diffractive exchange. Additional kinematic variables are Bjorken- x $x = \beta x_P$ and the inelasticity $y = Q^2/(sx)$ where s is the ep centre-of-mass energy squared.

The cross section is proportional to the combination of two structure functions:

$$\sigma \propto F_2^D - Y F_L^D \equiv \sigma_r^D, \quad (1)$$

where $Y = \frac{y^2}{1+(1-y)^2}$ is a kinematic factor resulting from the difference of the fluxes of transversely and longitudinally polarised photons from the electron. F_2^D is proportional to the diffractive γ^*p cross section, whereas F_L^D is related only to the part induced by longitudinal photons. The factor Y is sizable at large values of y and in most of the phase space measured so far, F_L^D is a small correction.

2. FACTORISATION IN DIFFRACTION

The diffractive structure functions have been proven to factorise into diffractive parton densities f_i^D of the proton convoluted with ordinary

*Talk presented at Diffraction 2004 Conference, Sardinia.

photon-parton scattering cross sections $\hat{\sigma}^{\gamma^* i}$ [1]:

$$F_2^D = \sum_i f_i^D \otimes \hat{\sigma}^{\gamma^* i}, \quad (2)$$

where the sum runs over all partons. This factorisation formula holds for large enough scales at leading twist and applies also to F_L^D . The diffractive parton densities obey the standard QCD evolution equations and can be determined from fits to structure function data.

3. EXPERIMENTAL RESULTS

3.1. Dependence on t

The t dependence of the cross section has the form $d\sigma/dt \propto e^{bt}$ with a slope parameter $b \approx 5$ to 7 GeV^{-2} which at the present level of precision does not depend on x_P as shown in Fig. 2 [2].

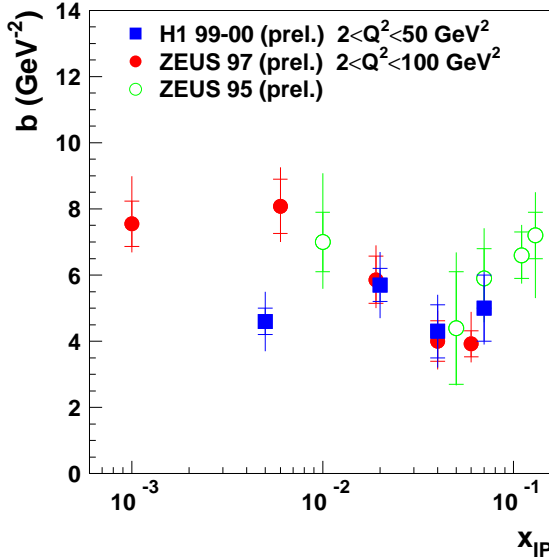


Figure 2. The slope parameter b from fits to the diffractive ep cross section $d\sigma/dt \propto e^{bt}$ for different values of x_P .

3.2. Dependence on x_P

The reduced diffractive cross section is shown in Fig. 3 as a function of x_P in bins of β and Q^2 . The measurements are obtained using a rapidity gap selection and cover a large kinematic range $Q^2 = 1.5$ to 1600 GeV^2 [3,4]. The collected event

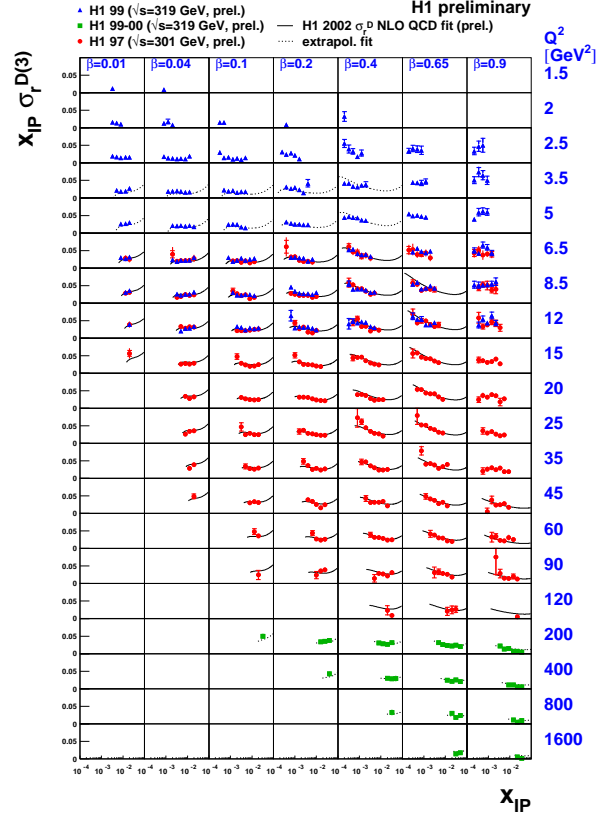


Figure 3. The reduced diffractive ep cross section $\sigma_r^D \equiv F_2^D - YF_L^D$ compared with the H1 2002 NLO QCD fit.

sample statistics do not allow an extraction of diffractive parton densities at fixed values of x_P . Instead, the x_P and t dependence of the PDFs are parameterised in a so-called flux factor f_P :

$$f_i^D(\beta, Q^2, x_P, t) = f_P(x_P, t) f_i^D(\beta, Q^2) \quad (3)$$

with $f_P(x_P, t) = e^{bt} x_P^{1-2\alpha_P(t)}$, where $\alpha_P(t) = \alpha_P(0) + \alpha'_P t$ is the linear pomeron Regge trajectory. This flux factor approach is consistent with the data within the present uncertainties for $x_P < 0.01$. At larger x_P values, a second term has to be introduced which can be interpreted as reggeon exchange:

$$\sigma_r^D = f_P (F_2^D + YF_L^D) + f_R (F_2^R + YF_L^R). \quad (4)$$

This is illustrated in Fig. 4 where the cross section is well described by f_P alone for $x_P < 0.01$. A fit to the data gives an intercept $\alpha_P(0) = 1.17^{+0.07}_{-0.05}$

which is larger than 1.08 as obtained for the soft pomeron in hadron-hadron collisions.

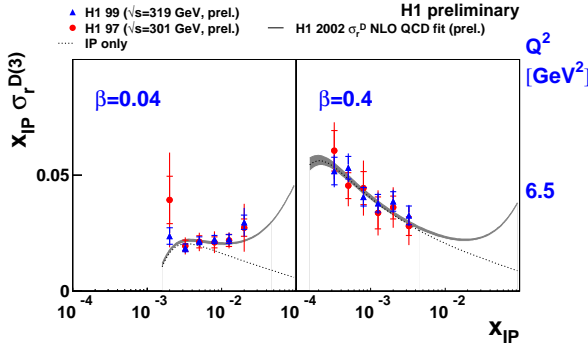


Figure 4. The $x_{\mathbb{P}}$ dependence of the reduced diffractive cross section for low and high β compared with the H1 2002 NLO QCD fit.

3.3. Scaling Properties and β dependence

The Q^2 and β dependences of the diffractive cross section are shown in Figs. 5 and 6 in a kinematic range ($y < 0.6$, $x_{\mathbb{P}} < 0.01$) where to good approximation $\sigma_r^D = F_2^D$ and the reggeon term is negligible. The shown data points display the pure β and Q^2 dependences of the structure function F_2^D ; kinematic effects related to $x_{\mathbb{P}}$ and t have been corrected by dividing the cross section by $f_{\mathbb{P}}$. In Fig. 5 the structure function displays approximate scaling for $\beta = 2/3$. For lower values the data exhibit scaling violations which are driven by a large gluonic component in the diffractive exchange. The structure function depends only weakly on β as shown in Fig. 6.

3.4. Diffractive parton densities

The H1 Collaboration has extracted diffractive parton densities from QCD fits to the diffractive structure function data. The $x_{\mathbb{P}}$ and t dependence of the PDFs is given by the flux factor as discussed in Sec. 3.2. The β dependences of the quark and gluon densities are parameterised at a starting scale $Q_0^2 = 3 \text{ GeV}^2$ and are evolved to the measured Q^2 values using the DGLAP equations [5]. The best fit is shown in Figs. 3–6 and describes the measurements very well. The corresponding parameterisations for the NLO and LO

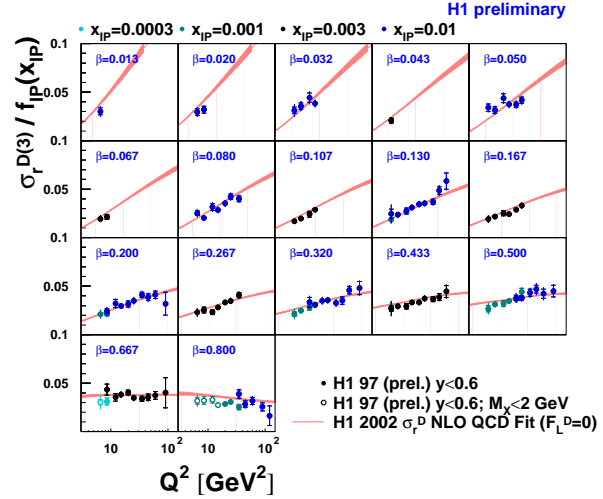


Figure 5. The diffractive structure function F_2^D as a function of Q^2 compared with the H1 2002 NLO QCD fit. The $x_{\mathbb{P}}$ dependence has been divided out.

quark and gluon densities are shown in Fig. 7. The gluon carries $\approx 75\%$ of the momentum of the diffractive exchange. The error band around the NLO densities includes experimental (inner band) and model uncertainties (outer band) which have been propagated to the PDFs. The gluon density is known to better than 30% up to fractional momenta $z \approx 0.5$, but is poorly known at large z . These densities have been used to predict diffractive final state cross sections such as dijet and heavy flavour production at HERA [6] and at the Tevatron [3].

3.5. Ratio of diffractive to inclusive cross section

The ratio of the diffractive to the inclusive cross section at the same $x = \beta x_{\mathbb{P}}$ is shown in Fig. 8 for $x_{\mathbb{P}} = 0.01$ as a function of Q^2 . For this particular $x_{\mathbb{P}}$ and the corresponding gap size, the diffractive contribution amounts to 2–3% of the inclusive cross section. The ratio is flat for $\beta < 0.6$ indicating a similar QCD evolution of the inclusive and the diffractive structure functions away from the kinematic limit $\beta = 1$ [3].

3.6. Charged current cross section

Diffractive processes which occur via W boson exchange instead of photon exchange have been

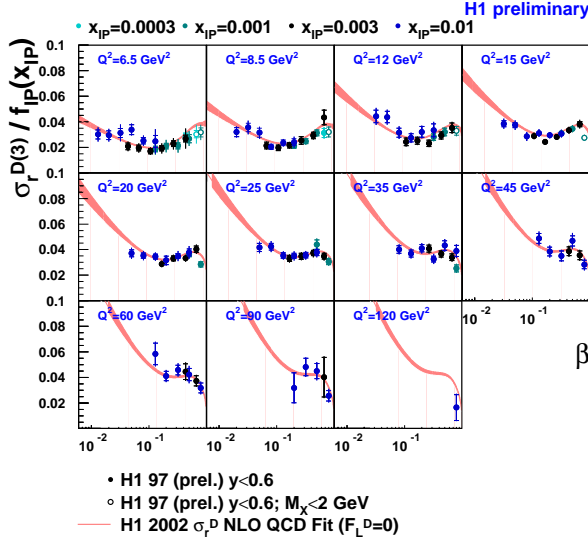


Figure 6. The diffractive structure function F_2^D as a function of β compared with the H1 2002 NLO QCD fit. The x_P dependence has been divided out.

measured by H1 using events with missing transverse energy which is carried away by the neutrino [7]. The ratio of the diffractive to the inclusive charged current cross section was measured to be $2.5\% \pm 1.0\%$ for $x_P < 0.05$. The cross section as a function of β is shown in Fig. 9. It is well described by a leading order Monte Carlo prediction which is based on the diffractive parton densities extracted in neutral current processes.

4. CONCLUSIONS

Diffractive structure functions have been measured by the H1 Collaboration to unprecedented precision. The data are consistent with QCD factorisation and diffractive parton densities have been extracted in QCD evolution fits. The gluon component carries $\approx 75\%$ of the momentum of the diffractive exchange. QCD factorisation was tested in diffractive charged current interactions where predictions based on the neutral current PDFs are in good agreement with the measured cross section. Diffractive and inclusive deep-inelastic ep scattering were shown to evolve similarly with the hard QCD scale.

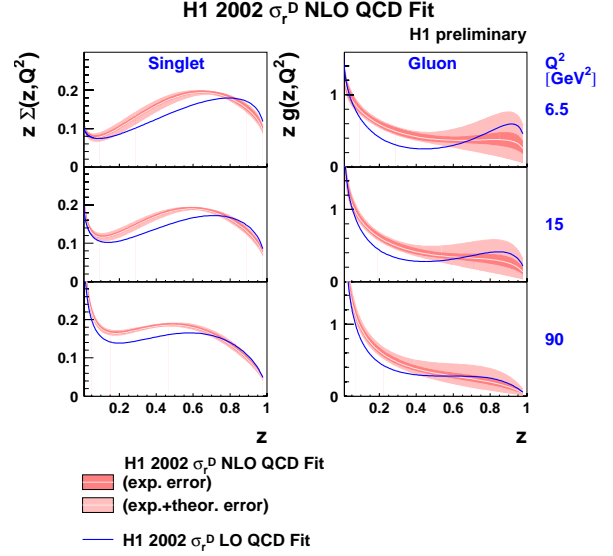


Figure 7. The H1 diffractive quark and gluon densities as extracted in a QCD fit to structure function data.

Acknowledgements

I thank my colleagues in H1 for their work reflected in this article and the organisers for an interesting conference in a splendid location. I thank Nicholas Malden for a thorough reading of the manuscript.

REFERENCES

1. J. Collins, *Phys. Rev. D* **57** (1998) 3051 and erratum ibid. **D61** (2000) 019902.
2. H1 Collaboration, paper 984 subm. to ICHEP 2002.
3. H1 Collaboration, paper 980 subm. to ICHEP 2002.
4. H1 Collaboration, paper 981 subm. to ICHEP 2002; H1 Collaboration, paper 6-0175 subm. to ICHEP 2004.
5. V. Gribov, L. Lipatov, *Sov. J. Nucl. Phys.* **15** (1972) 438, 675; Y. Dokshitzer, *Sov. Phys. JETP* **46** (1977) 641; G. Altarelli, G. Parisi, *Nucl. Phys. B* **126** (1977) 298.
6. H1 Collaboration, paper 6-0177 subm. to ICHEP 2004; H1 Collaboration, paper 6-0178 subm. to ICHEP 2004.
7. H1 Collaboration, paper 6-0821 subm. to ICHEP 2004.

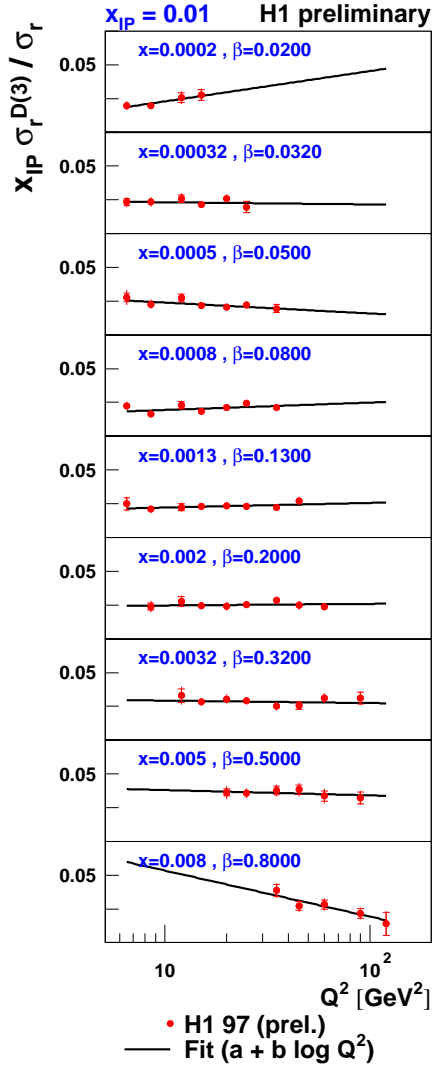


Figure 8. The ratio of diffractive to inclusive ep scattering cross sections as a function of Q^2 at $x_{IP} = 0.01$ for different values of $x = \beta x_{IP}$.

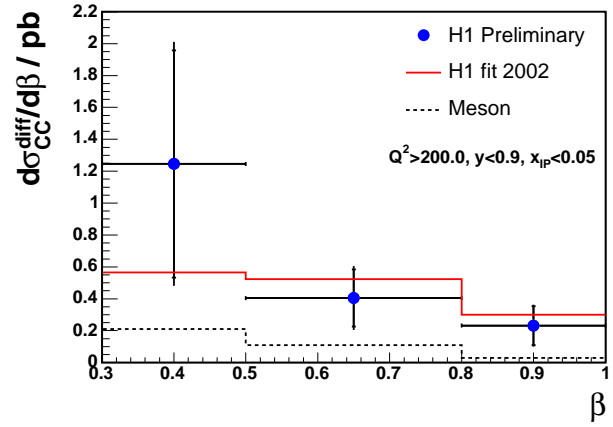


Figure 9. The diffractive charged current cross section as a function of the momentum fraction β compared with a LO prediction based on the LO diffractive parton densities of Fig. 7.